Generation of Bragg solitons through modulation instability in a Bragg grating structure

K. Porsezian[a)]
Department of Physics, Pondicherry University, Pondicherry-605 014, India

K. Senthilnathan[b)]
Department of Physics, Anna University, Chennai-600 025, India

(Received 10 December 2004; accepted 14 March 2005; published online 21 October 2005)

In this article, we consider the continuous wave (cw) propagation through the nonlinear periodic structure that consists of alternating layers of both positive and negative Kerr coefficients along the propagation direction. We investigate the modulational instability (MI) conditions required for the generation of ultrashort pulses for the nonlinearity management system. We study the occurrence of MI at the top and bottom edges of the photonic band gap (PBG) where the forward and backward propagating waves are strongly coupled because of the presence of the grating structure. We also study the MI when cw is detuned from the edges of the PBG into the anomalous and normal dispersion regimes. In addition, we discuss the existence of gap solitons for the nonlinearity management system in the upper and lower branches of the dispersion curve through the MI gain spectra. We observe the generation of higher order solitons in the nonlinear periodic structure when the input power is increased beyond a certain critical level. Finally, we discuss the generation of higher order Bragg grating solitons through the intensity evolution of the forward and backward propagating fields. © *2005 American Institute of Physics*. [DOI: 10.1063/1.1899824]

Optical transmission using a short optical pulse is a fundamental technology for accomplishing a high speed and long distance global network. Among many optical transmission formats, an optical soliton offers a great potential to realize an advanced optical transmission system. For instance, in the field of nonlinear optics, soliton is generated after the exact balance between the group velocity dispersion and the fiber Kerr nonlinearity called self-phase modulation (SPM). To realize solitons in fiber, fibers of length of about hundreds of kilometers are required in order that dispersion counteracts with SPM. In recent times, scientists have been able to generate solitons in so-called fiber Bragg gratings (FBGs) whose length will be of the order of a few centimeters. This is mainly because of the grating induced dispersion which is six orders of magnitude greater than that of the conventional standard telecommunication fiber. In FBG, the solitons arise as a result of grating induced dispersion and Kerr nonlinearity. It should be emphasized at this juncture that just because the dispersion is many orders of magnitude larger than that of glass, the interaction lengths are reduced accordingly, enabling nonlinear pulse compression as well as soliton generation and soliton dynamics to be studied on length scales of centimeters. Moreover, these solitons have the ability to propagate through the grating structure with velocities that can be substantially less than that of the velocity of light in a pure glass without dispersive broadening. Realizing the importance of generation of solitons in Bragg grating structure, this article attempts to address the generation of ultrashort pulses through MI phenomenon.

I. INTRODUCTION

In recent times, there has been renewed interest in modulational instability (MI) studies in both fiber and periodic structure in fiber known as fiber Bragg grating, because of its fundamental and applied interests.[1–3] It is well established that when the input is a light pulse, the propagation in an optical fiber is governed by the well-known nonlinear Schrödinger (NLS) equation and the output can be described in terms of a set of solitons. The issue to be investigated in this article is, "*what would happen if the input light wave has continuous wave (cw) amplitude?*" When it propagates through a fiber, one can show that the input light wave becomes unstable for a small perturbation around the initial amplitude. This instability is called the modulational instability (MI), also known as Benjamin–Feir instability. This phenomenon was predicted by Benjamin and Feir[4] for waves on deep water and by Bespalov and Talanove[5] for electromagnetic waves in nonlinear media with cubic nonlinearity. It should be noted that the MI has been observed in many branches of physics such as nonlinear optics, plasma physics, and condensed matter physics (fibers, magnetics, BECs, long Josephson junction, etc.).

Note that the perturbation of a cw in the MI process can either originate from quantum noise or from a frequency shifted signal. In the time domain, induced MI leads to the break-up of the quasi-cw pump wave into a train of ultrashort pulses.[6] It has been shown that the temporal shape of these ultrashort pulses depends not only on the powers of the

[a)]Electronic mail: ponzsol@yahoo.com
[b)]Electronic mail: senthee12@rediffmail.com

different waves but also on the modulational frequency.[7] In the frequency domain, the generation of high-repetition-rate pulse trains resulting from MI is determined by the growth of a cascade of sidebands. The number of harmonics is given by the temporal shape of the generated pulses and is determined by the initial conditions at the fiber input.[7] Based on the field component involved in the MI process, MI is further classified into two types. The first one is the scalar MI involving a single pump wave propagating in a standard nonbirefringent fiber. The other one is known as the vector MI, which involves more than one field component. Vector MI occurs in a birefringent fiber due to cross-phase modulation (XPM) between two modes that extends the instability domain to the normal dispersion regime, which is in contrast to the result of the NLS equation. This vector MI is also called XPM induced MI.

The occurrence of MI in fibers was first suggested by Hasegawa and Brinkman.[8] Later it was experimentally verified by Tai, Hasegawa, and Tomita.[9] In addition, various higher order linear and nonlinear effects such as higher order dispersions, self-steepening, and time delayed Raman effects have also been considered and these effects are found to strongly influence MI in fibers.[1]

Like in the case of fiber, MI in a FBG has been studied at low and high power levels for both anomalous and normal group velocity dispersion (GVD) regimes in the upper and lower branches of the dispersion curve, respectively.[10] In the anomalous GVD case, at relatively low powers, the gain spectrum is found to be similar to the case of a uniform index fiber. MI also occurs even in the normal GVD case where MI has a threshold condition. Recently, MI has been observed experimentally in an apodized grating structure wherein a single pulse has been converted into a train of ultrashort pulses.[11,12] In addition to temporal instabilities, spatial temporal instabilities have also been studied in a nonlinear bulk medium with Bragg gratings in the presence of Kerr-type nonlinearity.[13] Very recently, in the dynamic grating, it has been experimentally shown that there is no power threshold for the occurrence of MI in the normal dispersion regime.[14,15]

In this article, we plan to discuss the MI-driven dynamics and their subsequent generation of ultrashort pulses near and away from the PBG structure for the nonlinearity management system under the influence of Kerr nonlinearity. We also discuss the generation of higher order Bragg grating solitons in the nonlinearity management system through MI gain spectra scheme. This article is laid out as follows. In Sec. II, we introduce the necessary and appropriate theoretical model to describe the nonlinear pulse propagation in the nonlinearity management system. We also explore the characteristics of the nonlinear periodic structure through the nonlinear dispersion relation in Sec. III. In Sec. IV, by applying the standard linear stability analysis, we investigate the occurrence of MI at the two edges of the photonic band gap structure as well as on the upper and lower branches of the dispersion curves. Section V deals with the discussion on the existence of bright and dark gap solitons derived from the various modulational instability conditions discussed in the previous section. In continuation of the analysis, in Sec. VI, we turn to discuss the generation of higher order solitons in the nonlinear periodic structure for both forward and backward propagating fields. Finally, we present conclusion of this article in Sec. VII.

II. THEORETICAL MODEL

In recent works, He *et al.*,[16] Brzozowski *et al.*,[17] and Pelinovsky *et al.*[18] have introduced the concept of nonlinearity management of refractive optical gratings by suitably compensating Kerr nonlinearities. This leads to the disappearance of multistability resulting in hysteresis free operation, and they have modeled a complete analytical theory of true all-optical limiting in nonlinear optical gratings.[19] Our present work deals with the study of the nonlinear cw solution and its destabilization of the above-mentioned model by utilizing the concept of MI.

Recently, Pelinovsky *et al.*[18,19] have arrived at the nonlinear coupled mode (NLCM) equations that govern the nonlinear pulse propagation in a nonlinear periodic structure consisting of N alternating layers with different linear refractive indices and different Kerr nonlinearities having the form[19]

$$\begin{aligned} &i\frac{\partial A_f}{\partial z}+\frac{i}{v_g}\frac{\partial A_f}{\partial t}+\delta A_f+\kappa A_b+\alpha(|A_f|^2+2|A_b|^2)A_f \\ &\quad+\beta[(2|A_f|^2+|A_b|^2)A_b+A_f^2A_b^*+A_b^2A_f^*]=0, \\ &-i\frac{\partial A_b}{\partial z}+\frac{i}{v_g}\frac{\partial A_b}{\partial t}+\delta A_b+\kappa A_f+\alpha(|A_b|^2+2|A_f|^2)A_b \\ &\quad+\beta[(2|A_b|^2+|A_f|^2)A_f+A_b^2A_f^*+A_f^2A_b^*]=0. \end{aligned} \tag{1}$$

Here z and t are the normalized spatial coordinate and time, respectively, and v_g is the group velocity. The parameters $\delta(=(\bar{n}/c)(\omega-\omega_B))$ and κ are the detuning and linear coupling coefficients, respectively. The parameters α and β are nonlinearity coefficients, β being the coefficient of nonlinearity management. When $\beta=0$, Eq. (1) reduces to the well-known NLCM equations for the conventional FBG having positive Kerr coefficients along the propagation direction, studied already extensively, in the literature.[10]

III. NONLINEAR DISPERSION RELATION

Before investigating the MI conditions, first we explore the characteristics of the nonlinear periodic structure in the presence of Kerr nonlinearity through the nonlinear dispersion relation. It has been well established that knowledge of the nonlinear dispersion curves obtained from the continuous wave solutions of the coupled-mode equations provide considerable physical insight into the existence of the photonic band gap.[2,10] In order to derive the nonlinear dispersion relation for the NLCM equations, we assume the following form of the solution:

$$A_f=u_f\exp(iqz), \quad A_b=u_b\exp(iqz), \tag{2}$$

where $q=k-k_B$ represents wave number, u_f and u_b are the constants along the grating length, expressed generally in terms of a parameter, $f=u_b/u_f$, which represents the ratio of

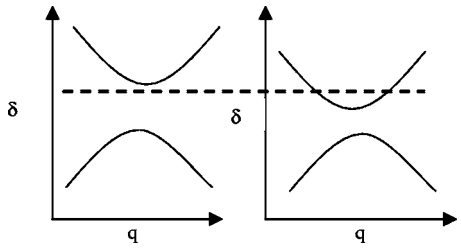

FIG. 1. At low field strengths, center frequency falls within the PBG (left). At high field strengths, the center frequency gets tuned out of the PBG.

the forward- to the backward-propagating waves. In other words, the parameter f describes how the total power $P_0 = u_f^2 + u_b^2$ is divided between the forward- and backward-propagating waves and hence can be written as

$$u_f = \sqrt{\frac{p_0}{1+f^2}}, \quad u_b = \sqrt{\frac{p_0}{1+f^2}} f. \tag{3}$$

Here, f can be positive or negative. For values of $|f| < 1.0$, the backward wave dominates. On substituting Eqs. (2) and (3) in the basic equation, the following dispersion relations can be arrived at:

$$q = -\kappa \frac{(1-f^2)}{2f} - \frac{\alpha P_0}{2} \frac{1-f^2}{1+f^2} - \beta P_0 \left(\frac{1+f-f^2}{2f} \right),$$
$$\delta = -\kappa \frac{(1+f^2)}{2f} - \frac{3\alpha P_0}{2} - \frac{\beta P_0}{2f} \frac{f^4+f^3+6f^2+1}{1+f^2}. \tag{4}$$

When $\beta = 0$ in Eq. (4), the dispersion relations for the case of FBG having the same positive Kerr coefficients can be retrieved.[10] When we introduce the positive/negative nonlinearity into the system, there is a corresponding increase/decrease in the average refractive index of the medium. This in turn shifts the center frequency from the middle of the band gap. It also means that the high intensity electric field shifts the PBG to either the upper or lower branches of the dispersion curves depending on the sign of nonlinearity. Thus positive nonlinearity shifts PBG down in energy and as a result the center frequency now locally gets tuned to the upper edge of the PBG. The negative nonlinearity shifts the PBG up in energy, and hence the central frequency is now shifted to the lower edge of the PBG. These events are clearly depicted in Fig. 1.

When the power of the applied electric field exceeds a certain threshold power called critical power, the applied field drastically affects the PBG. This critical value of P_0 can be calculated from the nonlinear dispersion relation (4). In order to study the role of nonlinearity management coefficient on the PBG structure, first we intend to study the physics behind the role of nonlinearity on PBG in the absence of nonlinearity management coefficient.[2] Whenever the applied input power P_0 exceeds the critical power, $P_C (= 2\kappa/\alpha)$, there is a formation of loop on the upper branch of the dispersion curve and is shown in Fig. 2(a). For the negative nonlinearity, the loop is formed on the lower branch, which is also shown in Fig. 2(b).

Introducing the nonlinearity management into the system ultimately reduces the size of the loop already formed. It can also be seen that increasing nonlinearity management further leads to the disappearance of the loop. The reason behind the same could be attributed to the fact that the more we introduce nonlinearity management, the more the system ceases to hold its nonlinear flavor and that is why dispersion curves resemble the case of the PBG of a linear case as shown in Figs. 2(c) and 2(d).

IV. LINEAR STABILITY ANALYSIS

The fundamental idea of linear stability analysis (LSA) is to perturb the cw solution slightly and then study whether this small perturbation grows or decays with propagation. It should be emphasized that LSA is valid as long as the perturbation amplitude remains small compared with the cw beam amplitude. If the perturbation amplitude grows large

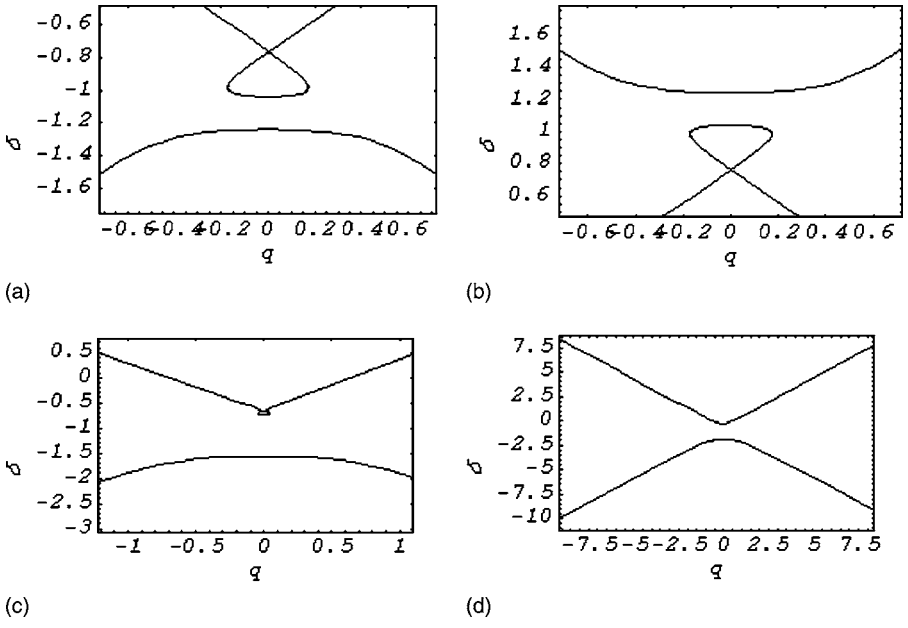

FIG. 2. (a) Role of positive nonlinearity on the PBG in the absence of nonlinearity management. (b) Role of negative nonlinearity on the PBG in the absence of nonlinearity management. (c) Role of nonlinearity management coefficient, when $\beta = 0.4$, on the PBG. (d) Role of nonlinearity management coefficient, when $\beta = 0.9$, on the PBG.

enough to be comparable to that of the incident cw beam, the numerical analysis must be adopted. In this section, we restrict ourselves to the former case. Here, we perturb slightly the steady-state solutions, given by Eq. (2), without imposing boundary conditions at the grating ends.[11] After the perturbation, Eq. (2) changes as

$$A_j = (u_j + a_j)\exp(iqz), \quad (j + f,b). \tag{5}$$

Assuming that the perturbation a_j is small, we substitute Eq. (5) into the basic equations and linearize in a_j to obtain

$$\begin{aligned} &i\left(\frac{\partial a_f}{\partial z} + \frac{1}{v_g}\frac{\partial a_f}{\partial t}\right) - \kappa f a_f + \kappa a_b + \frac{\alpha p_0}{1+f^2} \\ &\quad \times [a_f + a_f^* + 2f(a_b + a_b^*)] + \frac{\beta p_0}{1+f^2}\left[\frac{1}{2}a_f + 2a_b + a_b^* \right. \\ &\quad \left. + f(a_f + 2a_f^* + 2a_b) + f^2(2a_b + a_b^* + a_f^*) - f^3 a_b\right] = 0, \\ &-i\left(\frac{\partial a_b}{\partial z} - \frac{1}{v_g}\frac{\partial a_b}{\partial t}\right) - \frac{\kappa}{f}a_b + \kappa a_f + \frac{\alpha p_0}{1+f^2}[2f(a_f + a_f^*) + f^2(a_b \\ &\quad + a_b^*)] + \frac{\beta p_0}{1+f^2}\left[-\frac{1}{2}a_b + 2a_f + a_f^* \right. \\ &\quad \left. + f(a_b + 2a_f + 2a_b^*) + f^2(2a_f + a_f^* - a_b) - \frac{a_b}{f} + a_b^*\right] = 0. \end{aligned} \tag{6}$$

In order to solve the set of two linearized equations given by Eq. (6), we assume a plane wave ansatz, constituting both forward and backward propagation, having the form[2,10]

$$a_j = c_j \exp(i(Kz - \Omega t)) + d_j \exp(-i(Kz - \Omega t)) \quad (j = f,b), \tag{7}$$

where c_j and d_j are real constants, K the propagation constant, and Ω the perturbation frequency. Following the method discussed in Ref. 10, on substituting Eq. (7) into Eq. (6), we obtain a set of four homogeneous equations satisfied by c_j and d_j,

$$\begin{aligned} &\left(-K + s - \kappa f + \Gamma_1 + \Gamma_2 f(1-f^2) + \frac{\Gamma_2}{2}\right)c_f \\ &\quad + (\kappa + 2\Gamma_1 f + 2\Gamma_2(1+f^2) + 2\Gamma_2)c_b + (\Gamma_1 + \Gamma_2 f(2+f))d_f \\ &\quad + (2\Gamma_1 f + \Gamma_2(1+f^2))d_b = 0, \\ &(\kappa + 2\Gamma_1 f + 2\Gamma_2(1+f^2) + 2\Gamma_2)c_f \\ &\quad + \left(K + s - \frac{\kappa}{f} + \Gamma_1 f^2 - \frac{\Gamma_2}{2} - \frac{\Gamma_2}{f} + \Gamma_2 f(1-f)\right)c_b \\ &\quad + (2\Gamma_1 f + \Gamma_2(1+f^2))d_f + (\Gamma_1 f^2 + \Gamma_2(1+2f))d_b = 0, \\ &(\Gamma_1 + \Gamma_2 f(2+f))c_f + (2\Gamma_1 f + \Gamma_2(1+f^2))c_b \\ &\quad + \left(K - s - \kappa f + \Gamma_1 + \frac{\Gamma_2}{2} + \Gamma_2 f(1-f^2)\right)d_f \\ &\quad + (\kappa + 2\Gamma_1 f + 2\Gamma_2 + 2\Gamma_2(1+f^2))d_b = 0, \\ &(2\Gamma_1 f + \Gamma_2(1+f^2))c_f + (\Gamma_1 f^2 + \Gamma_2(1+f))c_b \\ &\quad + (\kappa + 2\Gamma_1 f + 2\Gamma_2 + 2\Gamma_2(1+f^2))d_f \\ &\quad + \left(-K - s - \frac{\kappa}{f} + \Gamma_1 f^2 - \frac{\Gamma_2}{2} - \frac{\Gamma_2}{f} + \Gamma_2 f(1-f)\right)d_b = 0. \end{aligned}$$

This set has a nontrivial solution if and only if the 4×4 determinant formed by the coefficients matrix vanishes as given in the following:

$$\begin{vmatrix} m_{11} & m_{12} & m_{13} & m_{14} \\ m_{21} & m_{22} & m_{23} & m_{24} \\ m_{31} & m_{32} & m_{33} & m_{34} \\ m_{41} & m_{42} & m_{43} & m_{44} \end{vmatrix} = 0, \tag{8}$$

where

$$\begin{aligned} m_{11} &= -K + s - \kappa f + \Gamma_1 + \Gamma_2 f(1-f^2) + \frac{\Gamma_2}{2}, \\ m_{12} &= \kappa + 2\Gamma_1 f + 2\Gamma_2(1+f^2) + 2\Gamma_2, \\ m_{13} &= \Gamma_1 + \Gamma_2 f(2+f), \\ m_{14} &= 2\Gamma_1 f + \Gamma_2(1+f^2), \\ m_{21} &= \kappa + 2\Gamma_1 f + 2\Gamma_2(1+f^2) + 2\Gamma_2, \\ m_{22} &= K + s - \frac{\kappa}{f} + \Gamma_1 f^2 - \frac{\Gamma_2}{2} - \frac{\Gamma_2}{f} + \Gamma_2 f(1-f), \\ m_{23} &= 2\Gamma_1 f + \Gamma_2(1+f^2), \\ m_{24} &= \Gamma_1 f^2 + \Gamma_2(1+2f), \\ m_{31} &= \Gamma_1 + \Gamma_2 f(2+f), \\ m_{32} &= 2\Gamma_1 f + \Gamma_2(1+f^2), \\ m_{33} &= K - s - \kappa f + \Gamma_1 + \frac{\Gamma_2}{2} + \Gamma_2 f(1-f^2), \\ m_{34} &= \kappa + 2\Gamma_1 f + 2\Gamma_2 + 2\Gamma_2(1+f^2), \\ m_{41} &= 2\Gamma_1 f + \Gamma_2(1+f^2), \\ m_{42} &= \Gamma_1 f^2 + \Gamma_2(1+f), \\ m_{43} &= \kappa + 2\Gamma_1 f + 2\Gamma_2 + 2\Gamma_2(1+f^2), \\ m_{44} &= -K - s - \frac{\kappa}{f} + \Gamma_1 f^2 - \frac{\Gamma_2}{2} - \frac{\Gamma_2}{f} + \Gamma_2 f(1-f). \end{aligned}$$

This condition leads to a fourth-order polynomial in $s = (\Omega/v_g)$ whose roots depend on K, κ, and P_0. The four roots of the polynomial in s determine the stability of the continuous wave solution. It is well established that MI occurs when there is an exponential growth in the amplitude of the perturbed wave, which in turn implies the existence of a nonvanishing imaginary part in the complex parameter s.[2,10] The

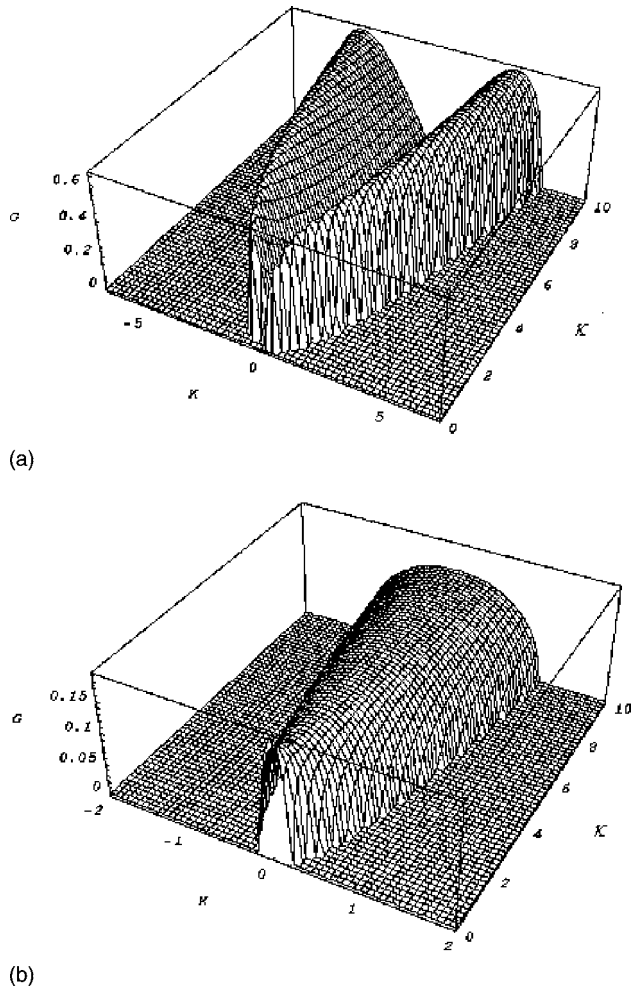

FIG. 3. (a) Gain spectrum in the anomalous dispersion regime, for the physical parameters: $P_0=0.1$, $\beta=0.001$, $\alpha=0.5$, and $f=-0.5$. (b) Gain spectrum in the anomalous dispersion regime, for the following physical parameters: $P_0=0.1$, $\beta=0.5$, $\alpha=0.5$, and $f=-0.5$.

MI phenomenon is measured by a gain given by $G \equiv |\mathrm{Im}\, s_m|$, where $\mathrm{Im}\, s_m$ denotes the imaginary part of s_m which is the root with the largest imaginary part. First we study the MI for the general case (where $f<0$ and $f>0$) and then consider the two more special cases when $f=\pm 1$.

A. The anomalous dispersion regime ($f<0$)

First we consider the general case where the parameter f with a value less than zero i.e., $f<0$, describes the detuning of the cw from the edge of the PBG into the anomalous dispersion regime. We obtain the gain spectra of MI for both the anomalous and normal dispersion regimes for the following two cases: (a) gain, $G(K,\kappa) \equiv |\mathrm{Im}\, sm(K,\kappa)|$ for a particular value of the input power P_0, and (b) $G(K,P_0) \equiv |\mathrm{Im}\, sm(K,P_0)|$ for a particular value of the linear coupling constant κ.

In the anomalous dispersion regime, for comparatively small values of the input power, say $P_0=0.1$ and nonlinearity management coefficient, say $\beta=0.001$, we obtain the gain spectrum having two distinct sidelobes on either side of zero propagation constant region and with a zero value along the line where the propagation constant vanishes. Also, the sidelobes broaden with increasing height as the value of the linear coupling coefficient κ increases as depicted in Fig. 3(a). For the same situation, but having comparatively large value of the nonlinearity management coefficient, say, $\beta=0.5$, the sidelobes vanish and, instead, we obtain a gain spectrum centered around the zero propagation constant region with a maximum value along the line where the propagation constant vanishes. Also, the centered lobe broadens with increasing κ, as is portrayed in the surface plot of Fig. 3(b).

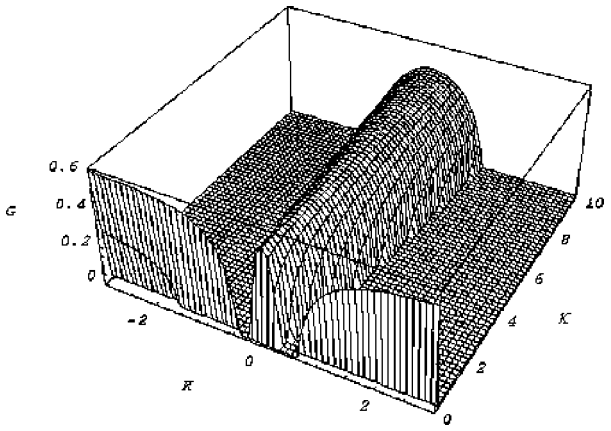

FIG. 4. Gain spectrum at the top of the PBG for the following physical parameters: $P_0=0.5$, $\beta=0.9$, $\alpha=0.5$, and $f=-1$.

B. Top of the photonic band gap ($f=-1$)

It is well known that the condition $f=-1$ represents the tuning of the cw into the top of the photonic band gap. Now on repeating the same procedure for $f=-1.0$, in addition to having a centered lobe, we observe two distinct curves whose heights reduce on either side of the zero propagation constant when the coupling coefficient κ is increased, which is as shown in Fig. 4.

C. The normal dispersion regime ($f>0$)

Now, we consider the other general case for which the parameter f is greater than zero i.e., $f>0$, which represents the detuning of the cw into the lower branch of the dispersion curve where the grating-induced dispersion is normal.

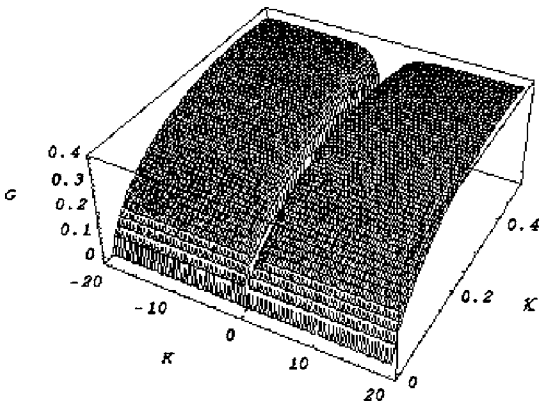

FIG. 5. Gain spectrum in the normal dispersion regime when $P_0=0.5$, $\beta=0.001$, $\alpha=0.5$, and $f=0.5$.

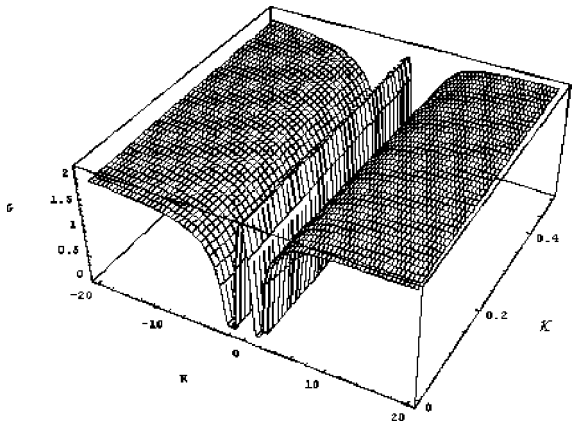

FIG. 6. Gain spectrum in the normal dispersion regime when $P_0=0.5$, $\beta=0.5$, $\alpha=0.5$, and $f=0.5$.

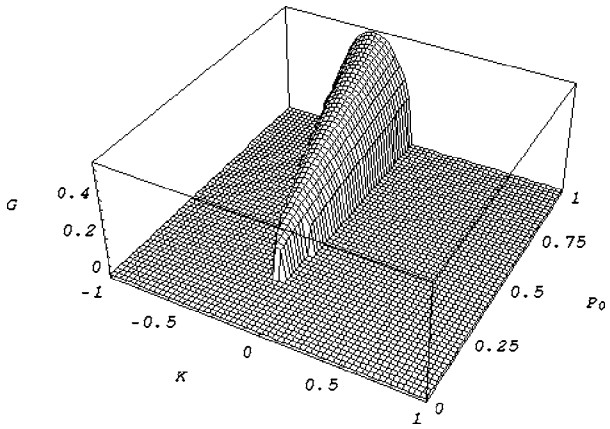

FIG. 8. Gain spectrum in the anomalous dispersion regime for various values of the input power P_0 and when $\beta=0.1$, $\alpha=1.4$, $\kappa=0.2$, and $f=-0.5$.

For the normal dispersion regime, for $f=0.5$ and for comparatively small values of the nonlinearity management coefficient, say $\beta=0.001$, the gain spectrum has values except along the line where the propagation constant vanishes which is shown in Fig. 5. For comparatively large values of the nonlinearity management coefficient, say $\beta=0.5$, the gain spectrum has a "w" shaped form centered around the zero propagation constant region and with the edges being flattened, as depicted in Fig. 6.

D. Bottom of the photonic band gap ($f=1$)

The condition $f=1$ corresponds to tuning the cw beam into the bottom of the photonic band gap. On repeating the same procedure for $f=1.0$, for comparatively small values of the (Nonlinear Management Coefficient) NMC, say $\beta=0.001$, the gain spectrum has zero value along the zero propagation constant region. However, it has maximum values along the line where the propagation constant vanishes for comparatively large values of the NMC, say $\beta=0.5$, and this is shown in Fig. 7. So far, we have plotted the gain spectrum by varying the linear coupling constant κ and keeping the input power P_0 fixed. Now on keeping the linear coupling constant κ fixed and on varying the input power P_0, we observe that the MI condition is achieved for comparatively small values of P_0 for both the anomalous and normal dispersion regimes. This is depicted in the surface plots given by Figs. 8 and 9.

Having discussed the MI gain spectra for both anomalous and normal dispersion regimes in the upper and lower branches of the dispersion curve for the nonlinearity management system, in Sec. V, we show the existence of the soliton in the upper and lower branches of the dispersion curve through the same physical parameter values for which the MI gain spectra have already been obtained.

V. DISCUSSION ON THE EXISTENCE OF GAP SOLITONS

The gap and Bragg solitons have been extensively investigated by many research groups in FBG and still the investigations on these exciting entities are alive. For instance, Chen and Mills[20] were the first to predict the existence of self-localization of a light wave within the (Photonic Band Gap) PBG of a nonlinear grating.

To investigate these solitons in FBG, so far, two theoretical approaches have been developed. The first one is the coupled mode theory which describes a coupling between

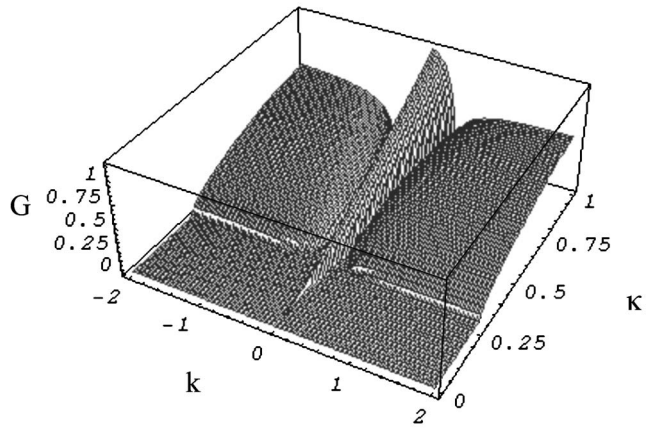

FIG. 7. Gain spectrum at the bottom of the PBG when $\beta=0.001$, $\alpha=1.4$, $\kappa=0.2$, and $f=1$.

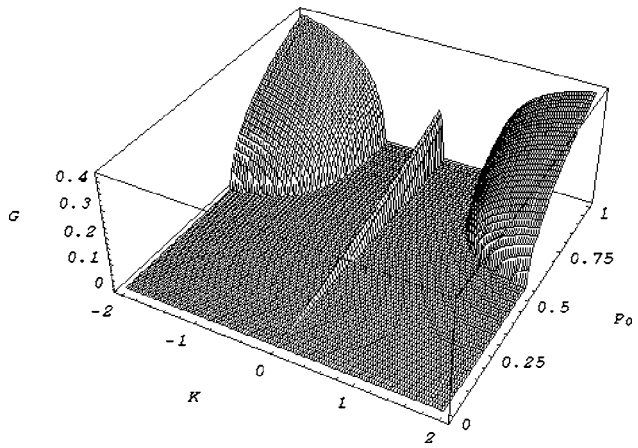

FIG. 9. Gain spectrum in the normal dispersion regime for various values of the input power P_0 and when $\beta=0.1$, $\alpha=1.4$, $\kappa=0.2$, and $f=0.5$.

forward and backward traveling modes where the nonlinear pulse propagation is described by the NLCM equations. In general, the NLCM equations are nonintegrable and are applicable anywhere in the PBG structure. However, in a few cases, NLCM equations have analytical solutions representing the solitary wave solutions. The most general form of the solitary wave solutions to the NLCM equations, for the first time, was derived by Aceves and Wabnitz.[21] It is to be noted that the most general solutions of Aceves and Wabnitz lead to the slow Bragg solitons, already predicted by Christodoulides and Joseph.[22]

The second one is the Bloch wave analysis, which is used to describe the nonlinear pulse propagation near the PBG structure. To achieve the same, usually a technique known as multiple scale analysis is adopted. Using the multiple scale analysis, Aceves[23] investigated the gap soliton bullets in the Kerr-type planar waveguides. Very recently, following the same multiple scale analysis, we have investigated the bright and dark solitons in FBG.[24]

At this juncture, we would like to show the generation of bright and dark solitons in the upper and lower branches of the dispersion curve through the MI gain spectra scheme. In order to show the existence of solitons in this periodic structure, we adopt a technique known as multiple scale analysis. In order to introduce the multiple scale analysis, we extend the linear solution to the following form:

$$\begin{pmatrix} A_f \\ A_b \end{pmatrix} = \varepsilon^{1/2} A(\tau_1, \tau_2, Z) \begin{pmatrix} 1 \\ -1 \end{pmatrix} e^{-i\kappa t} + \varepsilon U_1 + \varepsilon^{3/2} U_2 + \varepsilon^2 U_3 + \ldots, \tag{9}$$

where $\tau_1 = \varepsilon_t$, $\tau_2 = \varepsilon^2 t$, and $Z = \varepsilon^{1/2} z$. Now, we proceed to solve for (A_f, A_b) for successive orders in ε. Balancing the $O(\varepsilon)$ terms gives

$$LU_1 = -i \frac{\partial A}{\partial Z} \begin{pmatrix} 1 \\ 1 \end{pmatrix} e^{-i\kappa t}. \tag{10}$$

The solution of Eq. (10) is found to be

$$U_1 = -\frac{i}{2\kappa} \frac{\partial A}{\partial Z} \begin{pmatrix} 1 \\ 1 \end{pmatrix} e^{-i\kappa t}. \tag{11}$$

Next, we turn to compute the higher order corrections to (A_f, A_b). Balancing the $O(\varepsilon^{3/2})$ terms gives

$$LU_2 = \left(-i \frac{\partial A}{\partial \tau_1} - \frac{1}{2\kappa} \frac{\partial^2 A}{\partial Z^2} - (3\alpha - 5\beta)|A|^2 A \right) \begin{pmatrix} 1 \\ -1 \end{pmatrix} e^{-i\kappa t} + \text{c.c.} \tag{12}$$

In order to solve Eq. (12), the secular terms should be equated to zero and therefore,

$$i \frac{\partial A}{\partial \tau_1} + \frac{1}{2\kappa} \frac{\partial^2 A}{\partial Z^2} + (3\alpha - 5\beta)|A|^2 A = 0. \tag{13}$$

Equation (13) represents the pulse propagation outside the PBG structure. The variable E, in Eq. (13), represents the amplitude of the envelope associated with the Bloch wave formed by a superposition of E_f and E_b. For the first time, Sipe and Winful[25] derived this kind of NLS type equation from the NLCM equations. Sterke and Sipe[26,27] derived the NLS equation based on the envelope function approach and also presented the soliton solution outside the PBG structure. Without deriving the NLS equation from NLCM equations, Feng and Kneubuhl[28] investigated the formation of new types of solitary wave solutions called *out gap solitary wave solutions* in the periodic structure. Recently, Iizuka and Wadati[29] used reductive perturbation method and derived similar type of NLS equation in FBG. Recently, Aceves, in his recent work, considered higher order effects in FBG and hence derived perturbed NLS equation to describe gap soliton bullets in planar waveguides. In this article, we also consider the impact of higher order effects in FBG and derive the perturbed NLS equation. Then, we solve it for studying the formation of bright and dark Bragg solitons in both upper and lower branches of the dispersion curve in FBG. In order to study the impact of higher order effects, we continue to balance $O(\varepsilon^2)$ terms and this gives rise to

$$LU_3 = \left(i \frac{\alpha}{2\kappa} \left(2|A|^2 \frac{\partial A}{\partial Z} + A^2 \frac{\partial A^*}{\partial Z} \right) - \frac{i}{2\kappa} \left(-i \frac{\partial A}{\partial \tau_1} \right) \right) \times \begin{pmatrix} 1 \\ 1 \end{pmatrix} e^{-i\kappa t} + \text{c.c.} \tag{14}$$

Using Eq. (13), the equation for U_3 can be written as

$$U_3 = -\frac{i}{4\kappa^2} \left[(3\alpha - 5\beta) \left(2|A|^2 \frac{\partial A}{\partial Z} + A^2 \frac{\partial A^*}{\partial Z} \right) + \frac{1}{2\kappa} \frac{\partial^3 A}{\partial Z^3} \right] \times \begin{pmatrix} 1 \\ 1 \end{pmatrix} e^{-i\kappa t} + \text{c.c.} \tag{15}$$

Equation (15) represents the perturbation terms that must be added to the NLS equation when we consider the higher order effects in the FBG structure. With this result, the NLS equation changes into the (Perturbed Nonlinear Schrödinger) PNLS equation, which is presented in the following:

$$i \frac{\partial A}{\partial \tau_1} + \frac{1}{2\kappa} \frac{\partial^2 A}{\partial Z^2} + (3\alpha - 5\beta)|A|^2 A + \frac{1}{8\kappa^3} \frac{\partial^3 A}{\partial Z^3} + \frac{i}{4\kappa^2} (3\alpha - 5\beta) \left(2|A|^2 \frac{\partial A}{\partial Z} + A^2 \frac{\partial A^*}{\partial Z} \right) = 0. \tag{16}$$

It should be noted that, for the first time, Aceves derived this kind of PNLS equation in his recent work.[20] Here, we investigate bright and dark Bragg solitons with higher order effects at both upper and lower branches of the PBG.

Bright and dark bragg solitons. Here we will construct both bright and dark Bragg solitons for the PNLS equation that describes the nonlinear pulse propagation with higher order effects in the nonlinear periodic structure. Using the coupled amplitude-phase method, we solve the PNLS equation and discuss the generation of bright and dark Bragg solitons. For this purpose, we rewrite Eq. (16) in the form:

$$i \frac{\partial A}{\partial \tau_1} + a \frac{\partial^2 A}{\partial Z^2} + ib \frac{\partial^3 A}{\partial Z^3} + c|A|^2 A + id \left(4|A|^2 \frac{\partial A}{\partial Z} + 2A^2 \frac{\partial A^*}{\partial Z} \right) = 0, \tag{17}$$

$a = 1/2\kappa$, $b = 1/8\kappa^3$, $c = (3\alpha - 5\beta)$, *and* $d = (2\alpha - 5\beta)/4\kappa^2$. The coefficients a and b represent, namely, second- and third-

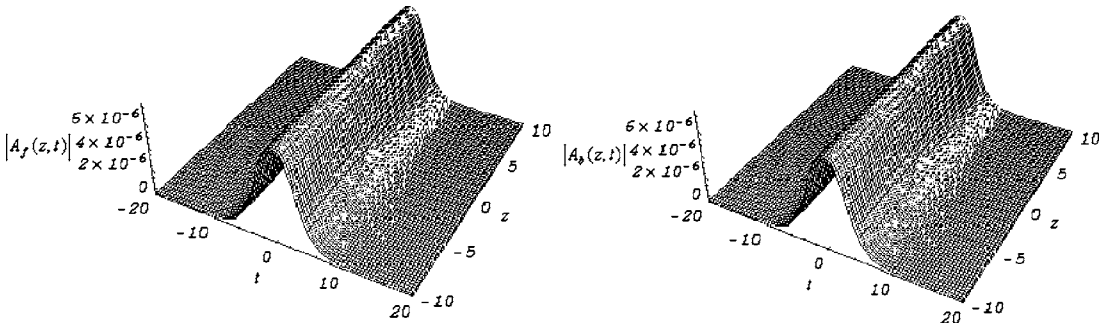

FIG. 10. Surface plot for the intensity of the bright one soliton (forward and backward propagating) when $P_0=0.05$, $\alpha=1.4$, $\beta=0.2$, $v_g=0.005$, $\kappa=0.2$, and $\varepsilon=10^{-4}$.

order dispersions. The parameter c is the nonlinear term representing the self-phase modulation. The last term in Eq. (17) accounts for self-steepening which results from including the first derivative of the slowly varying part of the nonlinear polarization. To solve Eq. (17), we consider the solution of the form[30]

$$A(z,\tau_1)=Q(\tau_1+v_g\xi)\exp[i(kZ-\omega\tau_1)], \tag{18}$$

where the function Q is a real one. The unknown parameters k and ω are directly related to the shifts in the wave number and frequency, respectively, while the factor v_g is the group velocity of the wave. Using Eq. (18) in Eq. (17) and removing the exponential term, we get

$$\begin{aligned} &iv_gQ_x-kQ+a[Q_{xx}-2i\omega Q_x \\ &\quad -Q\omega^2]+b[iQ_{xxx}+3\omega Q_{xx}-3i\omega^2Q_x-Q\omega^3]+cQ^3 \\ &\quad +d[3iQ^2Q_x+\omega Q^3]=0 \end{aligned}$$

Now, separating the real and imaginary parts, we have

$$v_gQ_\chi+bQ_{xxx}+(-2a\omega-3b\omega^2+3dQ^2)Q_x=0, \tag{19}$$

$$-kQ+(a+3b\omega)Q_{xx}+(c+d\omega)Q^3-(a\omega^2+b\omega^3)Q=0. \tag{20}$$

Since Eq. (19) possesses only third-order and first-order derivatives, it can be written in the following form:

$$bQ_{xxx}=(-v_g+2a\omega+3b\omega^2-3dQ^2)Q_x.$$

Integrating this, we get

$$Q_{xx}=\left(\frac{2a\omega+3b\omega^2-v_g}{b}\right)Q-\left(\frac{d}{b}\right)Q^3. \tag{21}$$

Writing Eq. (20) in the following form

$$Q_{xx}=\left(\frac{k+a\omega^2+b\omega^3}{a+3b\omega}\right)Q-\left(\frac{c+d\omega}{a+3b\omega}\right)Q^3. \tag{22}$$

It is clear that Eqs. (21) and (22) can be equivalent only under the following conditions:

$$\left(\frac{2a\omega+3b\omega^2-v_g}{b}\right)=\left(\frac{k+a\omega^2+b\omega^3}{a+3b\omega}\right),$$

$$\left(\frac{d}{b}\right)=\left(\frac{c+d\omega}{a+3b\omega}\right).$$

From the above-noted relations, we find ω and k as

$$\omega=\frac{cb-da}{2bd},$$

$$k=\frac{(2a\omega+3b\omega^2-v_g)(a+3b\omega)-ab\omega^2-b^2\omega^3}{b}. \tag{23}$$

Equation (21) can also be written as

$$d\chi=\frac{dQ}{\sqrt{\left(\frac{2a\omega+3b\omega^2-v_g}{b}\right)Q^2-\frac{1}{2}\left(\frac{d}{b}\right)Q^4+C}}, \tag{24}$$

where C is an arbitrary constant of integration. From Eq. (24), it is possible to get the different analytical solutions for different values of the constant of integration C. Among these solutions, we focus our attention on the solutions of bright and dark Bragg solitons. Now, we discuss how the bright soliton is formed outside the PBG but inside the FBG. Thereafter, we apply the same condition to the physical parameters in Eq. (24) and finally we obtain the bright soliton solution analytically. To discuss the bright soliton formation, we consider the self-focusing effect in FBG structure. Because of this effect, the central frequency of the carrier wave is tuned close to but outside the photonic band gap of the periodic structure. It physically means that the central frequency is moved to the upper branch of the dispersion curve,

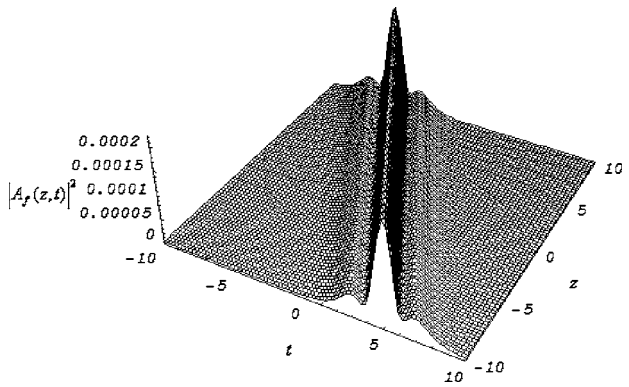

FIG. 11. Surface plot for the intensity of the bright two soliton (forward propagating) when $P_0=10.0$, $\alpha=1.4$, $\beta=0.2$, $v_g=0.005$, $\kappa=0.2$, and $\varepsilon=10^{-4}$.

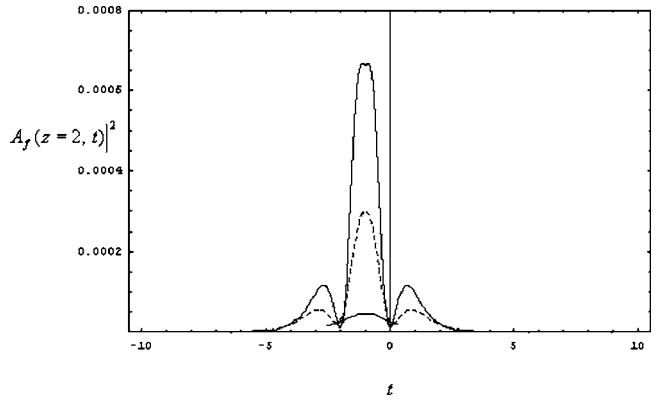

FIG. 12. Intensity plot of the bright one and two soliton for various input powers $P_0=0.2$ (dashed curve), $P_0=0.5$ (dotted curve), $P_0=0.7$ (solid curve).

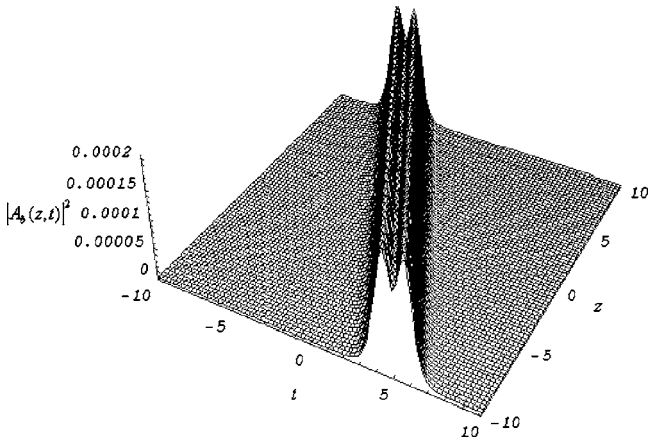

FIG. 13. Surface plot for the intensity of the bright two soliton (backward propagating) when $P_0=10.0$, $\alpha=1.4$, $\beta=0.2$, $v_g=0.005$, $\kappa=0.2$, and $\varepsilon=10^{-4}$.

where the grating induced group velocity dispersion (GVD) is anomalous. This anomalous GVD exactly gets balanced with the nonlinearity and, as a result, we have the bright soliton formation outside PBG but inside the periodic (FBG) structure, which is termed as *bright Bragg soliton*. As we consider positive nonlinearity in the formation of bright soliton, we choose the cubic nonlinear term as positive and $C=0$ in Eq. (24), and obtain the following bright soliton solution:

$$A=\sqrt{\frac{2(2a\omega+3b\omega^2-v_g)}{d}}\,\mathrm{sec}\,h\left(\sqrt{\frac{2a\omega+3b\omega^2-v_g}{b}}\right)\times\chi e^{i(kz-\omega\tau_1)}. \tag{25}$$

It should be noted that the existence of solitary waves in the upper branch of the dispersion curve has already been experimentally demonstrated.[31] Note that the formation of these solitons depends on the critical power of the MI gain spectra. From the MI gain spectrum of Fig. 8, we find that the critical power (P_c) is less than 0.2. Therefore, the bright soliton is formed in the upper branch (AD regime) for the input power $P_0>0.2$.

From the experimental point of view, it is necessary to know the magnitude of the peak power, P_0, to excite the bright Bragg soliton. Similarly, the soliton period, T_0, turns out to be another important physical parameter that is involved in the formation of Bragg soliton. From the bright Bragg soliton solution, we calculate the important and interesting physical parameters such as soliton power and pulse width in the form,

$$T_0=\sqrt{\frac{1}{(2a\omega+3b\omega^2-v_g)}},\quad P_0=\frac{2(2a\omega+3b\omega^2-v_g)}{d}.$$

With the known values of the parameters a, b, c, and d in a FBG, we can calculate ω using Eq. (23). After calculating the value of ω from Eq. (23), for a given T_0, we can easily calculate the value of β_1 from the above-presented relations. By computing all the physical parameter values, we can calculate the power required for generating the bright Bragg soliton. In addition, we have also found the relation connecting input power P_0 and pulse width T_0 as

$$T_0=\sqrt{\frac{2}{dP_0}}.$$

Similarly, there is another interesting class of solitons called dark solitons and now we discuss the formation of the same in the FBG. Instead of positive nonlinearity, we consider the negative nonlinearity, which gives rise to the self-defocusing effect in the FBG. This self-defocusing effect shifts the central frequency of the carrier wave to the lower branch of the dispersion curve where we have normal GVD. This normal GVD exactly gets balanced with the negative nonlinearity and as a result we get the dark soliton formation outside the PBG but inside the FBG structure. This soliton is referred to as *dark Bragg soliton*. For analytical purpose, considering the negative nonlinearity, the constant in Eq. (24) is chosen in such a way that the value of the expression inside the square root is a perfect square and hence we obtain the dark solitary wave solution as follows:

$$A=\sqrt{\frac{(2a\omega+3b\omega^2-v_g)}{d}}\,\tanh\left(\sqrt{\frac{2a\omega+3b\omega^2-v_g}{2b}}\right)\times\chi e^{i(kz-\omega\tau_1)}. \tag{26}$$

It should be emphasized that the dark soliton is formed in the lower branch for $P_0>0.25$ as we observe the critical power from the MI gain spectrum of the normal dispersion regime, which is nearly 0.25 as shown in Fig. 9. As has been discussed in the bright soliton case, it is also possible to calculate the power and pulse width for dark Bragg soliton case and the same are given in the following:

$$T_0=\sqrt{\frac{2}{(2a\omega+3b\omega^2-v_g)}},\quad P_0=\frac{(2a\omega+3b\omega^2-v_g)}{d}.$$

By knowing all the physical parameter values, one can calculate the power required to generate dark Bragg soliton.

VI. GENERATION OF HIGHER ORDER SOLITONS

Earlier in this article we discussed the generation of bright and dark solitons near the photonic band gap structures through the MI gain spectra scheme. In what follows,

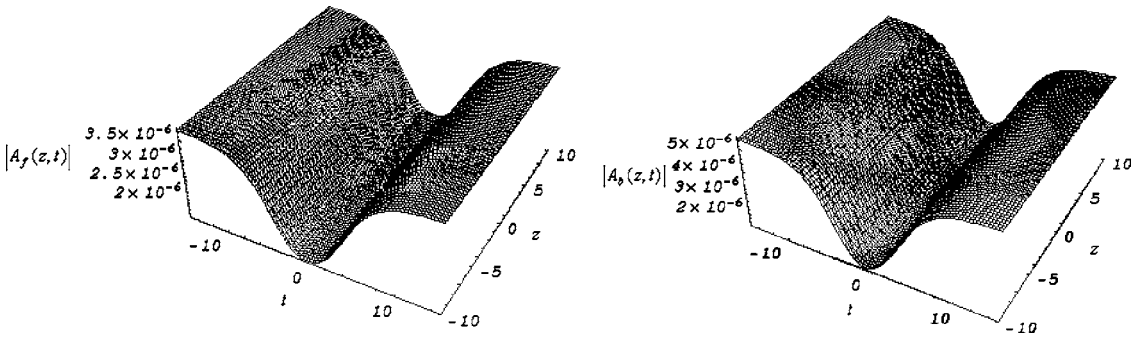

FIG. 14. Surface plot for the intensity of the dark one soliton (forward and backward propagating) when $P_0=0.045$, $\alpha=1.4$, $\beta=0.2$, $v_g=0.005$, $\kappa=0.2$, and $\varepsilon=10^{-4}$.

we turn to discuss the generation of higher order Bragg grating solitons for both forward and backward propagating modes near the photonic band gap structure. In order to study the intensity evolution of the forward and backward propagating waves in terms of nonstationary soliton solution in the nonlinear periodic structure, first, we find the values of the perturbation parameters U_1, U_2, and U_3. We note that these parameters have already been dealt with in our earlier studies.[24] The parameter U_1 is calculated as

$$U_1 = -\frac{i}{2\kappa}\frac{\partial A}{\partial Z}\begin{pmatrix}1\\1\end{pmatrix}e^{-i\kappa t}. \tag{27}$$

In the similar way, the parameter U_2 is calculated as

$$LU_2 = \left(-i\frac{\partial A}{\partial \tau_1} - \frac{1}{2\kappa}\frac{\partial^2 A}{\partial Z^2} - (3\alpha - 5\beta)|A|^2 A\right)\begin{pmatrix}1\\-1\end{pmatrix}e^{-i\kappa t} + \text{c.c.} \tag{28}$$

The expression for last parameter U_3 turns out to be

$$U_3 = -\frac{i}{4\kappa^2}\left[(3\alpha - 5\beta)\left(2|A|^2\frac{\partial A}{\partial Z} + A^2\frac{\partial A^*}{\partial Z}\right) + \frac{1}{2\kappa}\frac{\partial^3 A}{\partial Z^3}\right] \times\begin{pmatrix}1\\1\end{pmatrix}e^{-i\kappa t} + \text{c.c.} \tag{29}$$

Now, we discuss the forward and backward field intensity evolution in the nonlinear periodic structure by substituting the perturbation parameters U_1, U_2, U_3 and soliton envelope E obtained by Bloch wave analysis into Eq. (9). Here we consider the two cases for studying the forward and backward field evolutions as we have constructed both the bright and dark solitons. First, we consider the bright-soliton envelope for which we study the generation of higher order Bragg grating solitons in terms of the intensity of the forward field evolution. For comparatively low value of the input power, the formation of one soliton is observed. The bright one soliton in a periodic structure in terms of forward and backward field evolutions is clearly depicted in Fig. 10.

For a given value of v_g, as the input power increases beyond a certain power level, the influence of the nonlinear effects in the system is not negligible and hence plays an indispensable role in the formation of higher order bright solitons. For instance, the formation of two soliton is observed when the input power P_0 is 0.2 and during this process amplification as well as compression occurs. This is clearly shown in Fig. 11. It is interesting to note that this physical process is the same as pointed out by Mollenauer *et al.*[32] Now, by fixing the value of input power and on decreasing the value of coupling parameter κ, compression and amplification take place for corresponding changes in the value of κ. We also study the generation of higher order solitons for forward propagating field for various values of the input power.

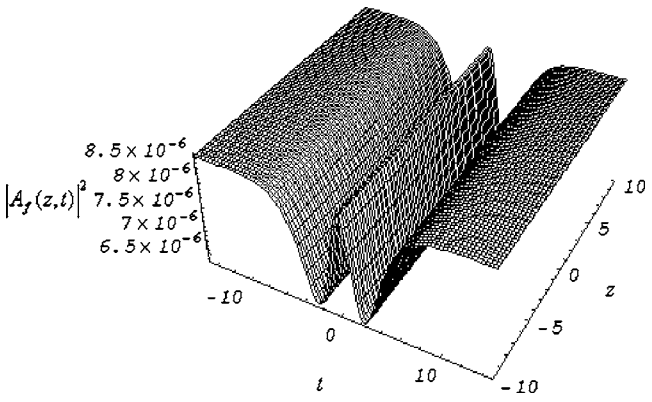

FIG. 15. Surface plot for the intensity of the dark two soliton (forward propagating) when $P_0=10.0$, $\alpha=1.4$, $\beta=0.2$, $v_g=0.005$, $\kappa=0.2$, and $\varepsilon=10^{-4}$.

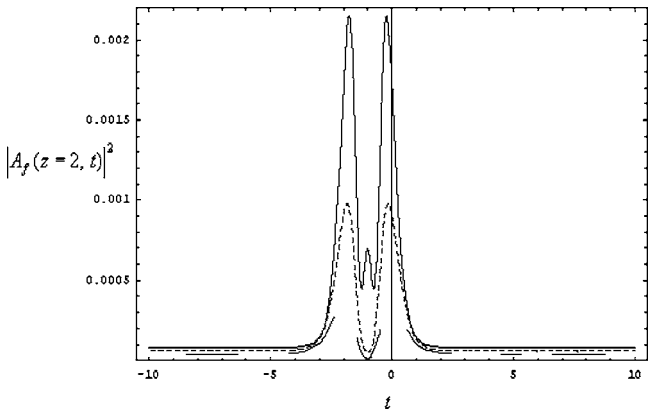

FIG. 16. Intensity plot of the dark one soliton for various input power $P_0=0.2$ (dashed curve), $P_0=0.5$ (dotted curve), $P_0=0.7$ (solid curve).

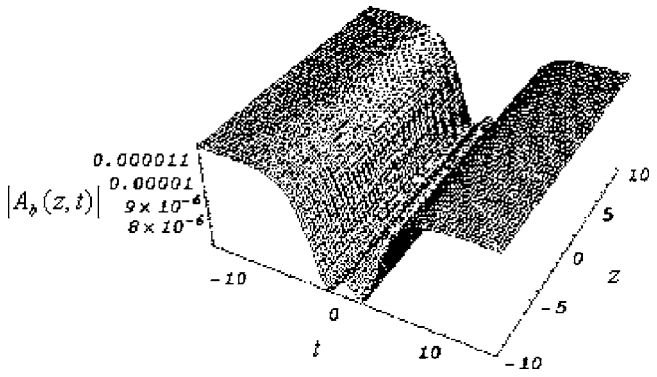

FIG. 17. Surface plot for the intensity of the dark two soliton (backward propagating) when $P_0=10.0$, $\alpha=1.4$, $\beta=0.2$, $v_g=0.005$, $\kappa=0.2$, and $\varepsilon=10^{-4}$.

The corresponding intensity evolution two-dimensional (2D) plots for various values of the input power are as shown in Fig. 12. That is, Fig. 12 clearly depicts the generation of one and two bright solitons in the nonlinear periodic structure as the input power is increased. Similarly, surface plot for the evolution of the backward field has also been obtained for the same physical parameter values and is clearly depicted in Fig. 13. In the second case, we also carry out the above-presented analysis for the dark soliton profile. To do so, we substitute the dark soliton profile and the perturbation parameters into Eq. (9). As in the bright soliton case, in this case also, we observe the generation of higher order solitons for moderately high values of the input power. For instance, when the input power is moderately low, the formation of dark one soliton has been observed for both forward and backward fields which are clearly depicted in Fig. 14. As has been discussed in the bright soliton case, the generation of two soliton has been observed when the input is increased beyond a certain level, say $P_0=0.2$. For this case, the intensity surface plot of forward field evolution is shown in Fig. 15. Following the above-presented analysis, one can easily understand the variation of the intensity of the propagating fields with respect to input power, with the help of 2D intensity plots for various values of the input power. Figure 16 clearly shows the generation of higher order dark solitons. Similarly, the dark two-soliton generation in terms of backward field intensity is depicted in Fig. 17.

VII. CONCLUSION

In this article, the modulational instability conditions required for the generation of ultrashort pulses have been investigated in BG under the influence of Kerr nonlinearity for both the anomalous and normal dispersion regimes as well as at the edges of the photonic band gap. In addition, from the various MI gain spectra scheme, we have also discussed the formation of Bragg grating solitons near the band edge when the carrier frequency of the laser pulse is detuned to either upper or lower branch of the dispersion curve depending on the sign of nonlinearity. Hence the governing NLCM equations were reduced to NLS and PNLS type equations using the multiple scale analysis. The PNLS equation, which incorporates both the higher order dispersive effects and self-steepening effects, has been derived to analyze the impact of nonlinearity on the pulse propagation in FBG. From the PNLS equation, the generation of bright and dark Bragg solitary waves has been investigated by coupled-phase amplitude method. It should be noted that the generation of higher order solitons is observed as the input power is increased. Thus, we have also discussed the generation of higher order bright and dark solitons in terms of the forward and backward propagating fields in the nonlinear periodic structure. Based on the arguments, we believe that ultrashort pulses could be generated experimentally for various values of the input power as the physical parameters of the system are closely related to numerical studies of all optical limiting in the nonlinearity management system. We have found that there exists a relation between the total input power and the soliton pulse width, and observed that on increasing the total input power, the soliton pulse amplitude increases for both the anomalous and normal dispersion regimes and also gets compressed. Besides we have explored the characteristics of the nonlinear periodic structure in the presence of Kerr nonlinearity for the nonlinearity management system through the nonlinear dispersion relation by studying the shift of the PBG in both upper and lower branches of the dispersion curve. The stability of these generated solitons in the MI driven dynamics is considered to be another important and interesting issue which will be communicated later.

ACKNOWLEDGMENTS

K.P. expresses his thanks to the DST, CSIR, DAE-BRNS and UGC (Research Award) Government of India for financial support through research grants. K.S.N. wishes to acknowledge CSIR for the award of a SRF.

[1] G. P. Agrawal, *Nonlinear Fiber Optics*, 2nd ed. (Academic, New York, 2001).
[2] G. P. Agrawal, *Applications of Nonlinear Fiber Optics*, 2nd ed. (Academic, New York, 2001).
[3] Y. Kivshar and G. P. Agrawal, *Optical Solitons: From Fibers to Photonic Crystals* (Academic, New York, 2003).
[4] T. B. Benjamin and J. E. Feir, "The disintegration of wave trains on deep water," J. Fluid Mech. **27**, 417–430 (1967).
[5] V. I. Bespalov and V. I. Talanove, "Filamentary structure of light beams in nonlinear liquids," JETP Lett. **3**, 307–310 (1966).
[6] A. Hasegawa, "Generation of a train of soliton pulses by induced modulational instability," Opt. Lett. **9**, 288–290 (1984).
[7] G. Millot, E. Seve, S. Wabnitz, and J. M. Haelterman, "Observation of induced modulational polarization instabilities and pulse-train generation in the normal-dispersion regime of a birefringent optical fiber," J. Opt. Soc. Am. B **15**, 1266–1277 (1998).
[8] A. Hasegawa and W. F. Brinkman, "Tunable coherent IR and FIR sources utilizing modulational instability," IEEE J. Quantum Electron. **16**, 694–697 (1980).
[9] K. Tai, A. Hasegawa, and A. Tomita, "Observation of modulational instability in optical fibers," Phys. Rev. Lett. **56**, 135–138 (1986).
[10] C. M. de Sterke, "Theory of modulational instability in fiber Bragg gratings," J. Opt. Soc. Am. B **15**, 2660–2667 (1998).
[11] B. J. Eggleton, C. M. de Sterke, and R. E. Slusher, "Nonlinear pulse propagation in Bragg gratings," J. Opt. Soc. Am. B **14**, 2980–2993 (1997).
[12] B. J. Eggleton, C. M. de Sterke, A. B. Aceves, J. E. Sipe, T. A. Strasser, and R. E. Slusher, "Modulational instability and tunable multiple soliton generation in apodized fiber gratings," Opt. Commun. **149**, 267–271 (1998).

[13]N. M. Lichinitser, C. J. McKinstrie, C. M. de Sterke, and G. P. Agrawal, "Spatiotemporal instabilities in nonlinear bulk media with Bragg gratings," J. Opt. Soc. Am. B **18**, 45–54 (2001).
[14]S. Pitios, M. Haelterman, and G. Millot, "Bragg modulational instability induced by a dynamic grating in an optical fiber," Opt. Lett. **26**, 780–782 (2001).
[15]S. Pitios, M. Haelterman, and G. Millot, "Theoretical and experimental study of Bragg modulational instability in a dynamic fiber grating," J. Opt. Soc. Am. B **19**, 782–791 (2002).
[16]J. He and M. Cada, "Optical bistability in semiconductor periodic structures," IEEE J. Quantum Electron. **27**, 1182–1188 (1991).
[17]L. Brzozowski and E. H. Sargent, "Optical signal processing using nonlinear distributed feedback structures," IEEE J. Quantum Electron. **36**, 550–555 (2000).
[18]D. Pelinovsky, L. Brzozowski, and E. H. Sargent, "Transmission regimes of periodic nonlinear optical structures," Phys. Rev. E **62**, R4536–R4538 (2000).
[19]D. Pelinovsky, J. Sears, L. Brzozowski, and E. H. Sargent, "Stable all-optical limiting in nonlinear periodic structures. I. Analysis," J. Opt. Soc. Am. B **19**, 43–53 (2002).
[20]W. Chen and D. L. Mills, "Gap solitons and the nonlinear optical response of superlattices," Phys. Rev. Lett. **58**, 160–163 (1987).
[21]A. B. Aceves and S. Wabnitz, "Self-induced transparency solitons in nonlinear refractive periodic media," Phys. Lett. A **141**, 37–42 (1989).
[22]D. N. Christodoulides and R. I. Joseph, "Slow Bragg solitons in nonlinear periodic structures," Phys. Rev. Lett. **62**, 1746–1749 (1989).
[23]A. B. Aceves, "Mathematical modeling in fiber and waveguide grating structures," in *Recent Advances in Optical Solitons: Theory and Experiments* Vol. 613, edited by, K. Porsezian and V. C. Kuriakose, (Springer, Berlin, 2003), pp. 165–184.
[24]K. Senthilnathan, K. Porsezian, P. Ramesh Babu, and V. Santhanam, "Bright and dark Bragg solitons in a fiber Bragg grating," IEEE J. Quantum Electron. **39**, 1192–1197 (2003).
[25]J. E. Sipe and H. G. Winful, "Nonlinear Schrödinger solitons in periodic structure," Opt. Lett. **13**, 132–134 (1988).
[26]C. M. de Sterke and J. E. Sipe, "Envelope function approach for the electrodynamics of nonlinear periodic structures," Phys. Rev. A **38**, 5149–5165 (1988).
[27]C. M. de Sterke and J. E. Sipe, *Gap solitons*, in Progress in Optics. Vol. XXXIII, edited by E. Wolf (Elsevier, Amsterdam, 1994), Chap. 3, pp. 203–260.
[28]J. Feng and F. K. Kneubuhl, "Solitons in a periodic structure with Kerr nonlinearity," IEEE J. Quantum Electron. **29**, 590–597 (1992).
[29]T. Iizuka and M. Wadati, "Grating solitons in optical fiber," J. Phys. Soc. Jpn. **66**, 230–2313 (1997).
[30]B. J. Eggleton, R. E. Slusher, C. M. de Sterke, P. A. Krug, and J. E. Sipe, "Bragg grating solitons," Phys. Rev. Lett. **76**, 1627–1630 (1996).
[31]M. Du, K. Chan, and K. Chui, "A novel approach to solving the nonlinear Schrödinger equation by the coupled amplitude-phase formulation," IEEE J. Quantum Electron. **31**, 177–182 (1995).
[32]L. F. Mollenauer, R. H. Stolen, and J. P. Gordon, "Experimental observation of picosecond pulse narrowing and solitons in optical fibers," Phys. Rev. Lett. **45**, 1095–1098 (1980).